International Journal of Heat and Technology
Vol. 43, No. 1, February, 2025, pp. 112-124
Journal homepage: http://iieta.org/journals/ijht

# Numerical and Experimental Investigation into the Effects Combined of Hybrid Nanofluids and Micro-Finned Surfaces on Pool Boiling Heat Transfer Enhancement

Khudir Z. Zarrag[1], Firas B. Ismail[1,2,3], Laith J. Habeeb[4*], Tan E. Sann[1]

[1] Power Generation Unit, Institute of Power Engineering, Universiti Tenaga Nasional, Kajang 43000, Malaysia
[2] Faculty of Engineering, Sohar University, PO Box 44, Sohar PCI 311, Oman
[3] Engineering College, A1-Bayan University, Baghdad PO Box 6111, Iraq
[4] Training and Workshop Center, University of Technology- Iraq, Baghdad 10066, Iraq

Corresponding Author Email: Laith.J.Habeeb@uotechnology.edu.iq

Copyright: ©2025 The authors. This article is published by IIETA and is licensed under the CC BY 4.0 license (http://creativecommons.org/licenses/by/4.0/).

https://doi.org/10.18280/ijht.430113

**Received:** 17 December 2024
**Revised:** 3 February 2025
**Accepted:** 18 February 2025
**Available online:** 28 February 2025

***Keywords:***
*aluminum oxide, hybrid nanomaterials, micro fins, nanomaterials, pool boiling heat transfer*

**ABSTRACT**

The present paper examines the utilization of hybrid nanomaterials, $Al_2O_3$ + CuO and ZnO, and micro-fins as compound heat enhancement techniques to maximize pool boiling heat transfer efficiency. Numerical modeling and experimental measurements have been adopted as research methods to identify the heat transfer parameters in a pool boiling process. The utilization of micro-fins increases surface areas and reduces vapor film, whereas $Al_2O_3$ nanoparticles with a dispersed arrangement improve thermal conductivity and promote liquid nucleation sites, which also contributes to enhanced heat transfer. An acrylic pool and copper tube are used as pool boiling systems. The pool is 15 × 15 × 25 cm without the pool thickness. Nanoparticle hybrid $Al_2O_3$ composed of CuO and ZnO is then tested for its thermal and physicochemical characteristics. Thermal discharge from fins experienced a rise with the temperature reaching 34℃ in water + 0.1 wt% $Al_2O_3$+ 0.4 wt% CuO. As well as 35℃ in water + 0.25 wt% $Al_2O_3$ + 0.25 wt% CuO and up to 38℃. Conclude that nanomaterials have great effectiveness in thermal discharge and the transfer of thermal energy from the fins to the water that contains nanomaterials, as well as improving the condensation process in the pipes.

## 1. INTRODUCTION

Pool boiling heat transfer is one of the methods widely used in several fields of industry, but efficiency calls for development. Evidently, the incorporation of nanomaterials in boiling events has become a center of attention, which applies to the heat transfer rate improvement. Alumina $Al_2O_3$ nanoparticles are remarkable for their excellent thermal conductivity and stability, justifying their deservedness as the most potential Nano sized candidates to improve heat transfer.

Mehralizadeh et al. [1] focused on boiling heat transfer enhancement techniques. It compared, analyzed, and brought out the effect of nucleation sites on surface enhancement to heat transfer. The research demonstrated that the choice of such factors as surface structure and manufacturing techniques for fluid is very important, and it will help to look for future options that will expand the possibilities for safe vacuum distillation or vapor exposure of the fluids. Mukherjee et al. [2] investigated Fusion plasma-facing components (PFC), which are cooled by efficient cooling procedures to ensure the system's safe operation and/or smooth performance. The HV-type heat exchanger has been chosen for cooling of PFCs.

The application of nanofluid as a coolant in HV has pointed out its promising route, but other investigations are to be done to know its total viability. Mahmoud and Karayiannis [3] analyzed pool boiling heat transfer acceleration, exploring the absence of a full inspection on enhanced surfaces among the studies. It considers why it is hard to assess performance, if it should be more smooth or roughened, and what kind of liquid effects to incorporate. FC-72 cooling water data and substrate materials such as copper and silicon are enhanced by digitizing all the current pool boiling data. The work displays the complex effect of combining fluid and surface and emphasizes the importance of appraising enhanced surface efficiency. It also provides criteria for appraising the performance of purposing fluids at specific surfaces, which practice, would be beneficial both for academic and application purposes. Gajghate et al. [4] studied the boiling heat transfer efficacy, which is a challenge in distillation and pharmaceutical industries. The device employs a fiber laser scribing technology combined with the v-shaped and rectangular grooved copper surfaces made in $ZrO_2$ nanofluid media. Nanofluid and microstructure promoted to have an increased relative heat transfer coefficient of 41.48%, thus lowering the wall superheat. The numerical model outperforms experimental data in accordance with the trajectory obtained.

Sharma et al. [5] reported the performance of the Ag/ZnO fluid as a nanofluid in thermal property investigations. This includes critical heat flux (CHF) and heat transfer coefficient (HTC) at varying concentrations. The nanofluids incorporated a 15% enhancement in the thermal conductivity at 45℃ rather than that of DI water. The higher CHF and the higher HTC were obtained from the higher concentration. However, the concentration further above these values will cause the transfer of boiling heat transfer to be worse.

Ravi Babu et al. [6] studied a thermodynamic system's working depends on efficient heat movement, and this fluid selection is crucial. Nanofluids, new generation working media endowed with outstanding thermo-physics characteristics, attract growing attention all the time because of their marked thermal properties upgrades. The most recent investigations have dealt with the fabrication, examination, and adoption of convention, free convection, and boiling heat transport.

Moghadasi and Saffar [7] presented an application of spin-coating technique under distilled water boiling of distilled water under atmospheric pressure. The results are characterized by better surface roughness and porosity, additional nucleation site density with lower interconnection distances, and lower resource usage and process time. Sample 4, with the largest value of NSD and roughness, produced the maximum heat transfer of the range, which was recorded as 101.78 $W/cm^2$. HD As the superior surface characteristics of the micro/nanostructured coatings came into play, the condition of the heat transfer coefficient became better. Dadhich et al. [8] investigated heat transfer rates employed in the working fluids in different applications and systems in the heat production process that are most prevalent in the industry. A systematic literature review of 100 research papers majority of which were published in journals, was carried out as the source. The study looked back at the previous works that concentrated on new working fluids and the creation of new correlations between input and output parameters.

Moghadasi et al. [9] investigated pool boiling (PB), which is a core heat transfer mechanism that is implemented in most heat/energy conversion applications as a way of improving performance. Research efforts have been directed towards a reduction in CHF by means of modifying aspects of boiling surfaces. The review assesses the employment of metal oxide nanoparticles as CHF improvers. Create your own unique skills box in 6 easy steps: The effects of nanoparticle material, thermodynamic properties of thermal properties, the concentration, the shape, and the size are categorized. Nanoparticle deposition is introduced as a replacement boiling nanofluid physical process, and mechanisms to explain the result are exhibited later on.

Soleimani et al. [10] created heat distribution techniques targeting high-heat devices as the latter are utilized effectively only by small, scale equipment. A poor heat transfer coefficient shows an over-prediction of local temperature, resulting in the possibility of an inaccurate temperature map. The writing concerns the thermal boundary layer used in the analysis of boiling as well as the bulb movement in the gas phase as the parameters that influence the heat transfer rate in flow boiling and disparity to the single-phase flow. This study found that using general-purpose synthetic base oils containing alumina nanoparticles potency was not achieved compared with copper-molybdenum-tin-zinc (Cu-Mo-Sn-Zn) additive. Mukesh Kumar and Arun Kumar [11] analyzed the performance of electronic chips in a heat sink made out of six channels of water and two fluids- $Al_2O_3$/water as heat sinks. The results reduce surface temperature, thermal resistance, power consumption and Nusselt number by 120%. The reliability is also improved by 20%. Mehralizadeh et al. [12] determined the effect of $TiO_2$ and $SiO_2$ Nanoparticles on the nanofluid HTC using numerical analysis. Converting initial results, it is evident that the system with a higher heat transfer coefficient provides these values bigger and it is more efficient. In addition, in the investigation, the result of surface modification, which was a covering with circular channels and intersections with lines, is the development of the efficiency of HTC for all of the nanofluids. The review not only engineered predictive methods utilizing the artificial neural network and adaptive neuro-fuzzy inference systems but also.

Khan et al. [13] focused on nucleate boiling, which is a phase change mechanism applied in a range of applications, such as steam power plants, thermal desalination, heat pipes, and waste heat recovery. The recently introduced micro/nanoscale surface nanotechnology applications and materials improvements, with purified geometric and chemical surface properties, are creating a new level of bubble nucleation and, thus, heat transfer enhancement. The surface coatings' materials are notably more flexible, straightforward, and resistant to environmental influences, thus making them useful to existing systems. It is a topic, which covers modern application of the particular methods and prospects of their employment in a real industry. Das et al. [14] studied and reported nano-porous composite media to better heat transfer during boiling. It focuses on studies of boiling in experiments with the wetting of service (the contact angle between the liquid-vapor interface and heating surface surface) also being under consideration as a possible factor. In addition, the work focuses on the different fabrication ways of the nano-coated heated surfaces while emphasizing the specific topography of boiling heat transfer, which is dependent on the active nucleation sites, bubble frequency, and morphology.

Qi et al. [15] focused on modeling of heat transfer boiling of nanofluid using a blend model and experimental investigations. The heat transfer roasting analysis of TiO2-water nanofluid performed using numerical and experimental methods is addressed. The results demonstrate that nanoparticles, when added to the water, increase the boiling heat transfer by 77.7% when applied in a ratio below 2% while increasing it by 30.3% when used in a higher mass fraction. The rising boiling heat transfer coefficients exhibit this characteristic.

Jaswal et al. [16] investigated pool boiling on three test surfaces: There are three main types of finned surfaces, namely Plain fins, Rectangular fins, and Trapezoidal fins. Analytical and numerical investigations were made to examine the fin spacing and height influences. It was ascertained that the heat flux values were enhanced. Experimental results showed that using rectangular and trapezoidal finned surfaces improved the heat flux values by 52.3% and 101.5%, respectively, compared to the plain surface. It incorporates the type of surface and availability of area through the heat transfer coefficient. Greater fin height enhancement was noted.

Alshuhail [17] reported that pool boiling in refrigeration and power plants benefits from nanofluids for enhanced thermal conductivity and heat transfer rates. This paper discusses nanofluids' characteristics in pool boiling heat transfer.

This study aimed to determine the improvement of pool boiling heat transfer efficiency using compound nanofluid and micro-fins. Hybrid nanofluids are formed by adding nana particles of $Al_2O_3$, CuO, ZnO to water and micro-finned surfaces. Various material compositions with varying weight percentages of $Al_2O_3$, CuO, and ZnO are examined. In addition, various micro-fin geometries for heaters are considered.

The investigation method included experimental and numerical analysis. Additional investigations have been performed utilizing ANSYS software to corroborate the experiment results as well as to predict the temperature fields and flow patterns using CFD simulation.

The significance of the results includes improved pool boiling heat transfer rates with the resultant use of hybrid nanofluids and better control of temperature distribution and thermal conductivity experienced in micro-fin structures. The work contributed to enhancing energy efficient cooling systems for industries.

The results of the work hold some novel findings in terms of offering a combination of hybrid nanofluids $Al_2O_3$, CuO, and ZnO in water, with micro-fin on pool boiling heat transfer performance. Unlike other studies that only employ a numerical model, method approach, or experimental technique, this paper presents both an experimental analysis and numerical validation results for obtaining exact fluid dynamics, thermal characteristics, and heat transfer on pool boiling systems. The results highlighted show the possibility of future high-performance thermal management systems, especially in energy applications.

## 2. METHODOLOGY

The process of pool boiling heat transfer in industrial applications such as cooling and heat production systems is of crucial importance. Scientists are working on getting hybrid nanomaterials and micro fins together in an attempt to increase efficiency. With incredible ability, members of family hybrid nanomaterials, such as $Al_2O_3$ nanoparticles, have been proven to be a powerful element for heat transfer. Booster fins, which are tiny protrusions on the surface area, in particular, can be used in the context of convective heat transfer.

### 2.1 Experimental implementation

2.1.1 Experimental setup

An acrylic boiling pool of size 150×150 mm and a height of 250 mm is prepared with demineralized water and equipped with microcontrollers for temperature control with heaters and flow meters. A heater made out of aluminum material was manufactured with 50×50 mm and a height of 10 mm. Four holes were drilled into the four cylindrical four heaters, whose temperature reached 150°C, and installed inside the metal piece to gain the desired heater's highly efficient heating. Type K thermal sensors are used, which are connected to the Arduino to program the sensor to record measured data. The heat dispersal of the outer object was incredible due to the large surface area. The openings of the lower part are completely covered by thermal insulation material to make sure that water does not enter. The experimental set up is described in many in Figure 1. Figure 1(a) shows the schematic of the setup, the measurement strategy, an electrical diagram, and the sensors used for the variables measurements. Figures 1(b) and 1(c) show details of the boiling unit and the locations of temperature measurements.

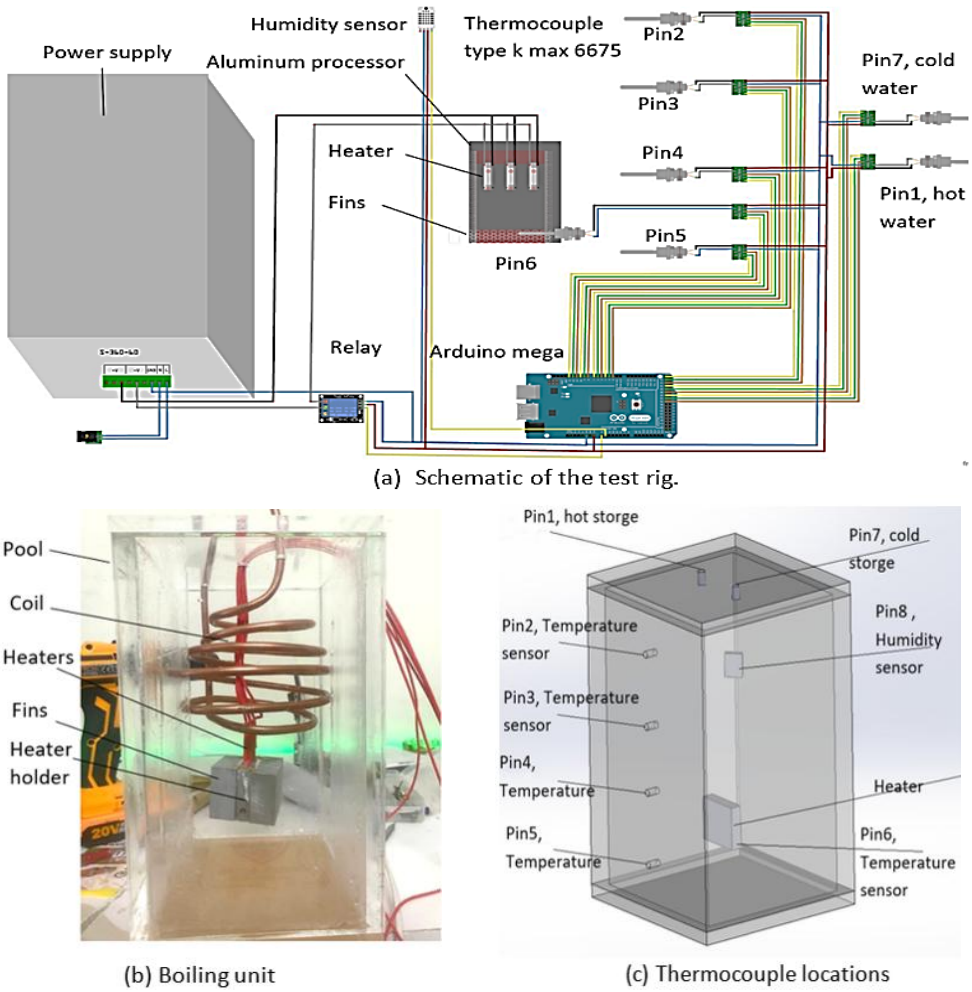


**Figure 1.** Pool boiling experimental setup and measurement system, (a) schematic of the rig, (b) boiling unit in the test rig, (c) thermocouples and their location

**Table 1.** Material properties

| Composition of Materials | Property | | | |
|---|---|---|---|---|
| | Density (kg/m$^3$) | Thermal Conductivity (W/m·K) | Specific Heat (J/kg·K) | Weight (g) |
| Water | 998.2 | 0.6 | 4182 | - |
| $Al_2O_3$ | 3970 | 17.65 | 525 | - |
| CuO | 6500 | 18 | 540 | - |
| ZnO | 5606 | 19 | 544 | - |
| Water+0.1 wt% $Al_2O_3$ + 0.4 wt% CuO | 1023 | 0.6866 | 4163.79 | 82 |
| Water+0.25 wt% $Al_2O_3$ + 0.25 wt% CuO | 1019 | 0.6861 | 4163.77 | 71 |
| Water+0.4 wt% $Al_2O_3$ + 0.1 wt% CuO | 1015 | 0.6856 | 4163.74 | 61 |
| Water+0.1 wt% $Al_2O_3$ + 0.4 wt% ZnO | 1023 | 0.6866 | 4163.79 | 72 |
| Water+0.25 wt% $Al_2O_3$ + 0.25 wt% ZnO | 1017 | 0.6886 | 4163.78 | 65 |
| Water+0.4 wt% $Al_2O_3$ + 0.1 wt% ZnO | 1014 | 0.6866 | 4163.75 | 58 |

All sets of thermocouple wires and sensors have been calibrated prior to usage for the experimental measurements. A sample of the calibration curve is shown in Figure 2. It represents a sample of the calibration of the temperature sensors before commencing the experiment.

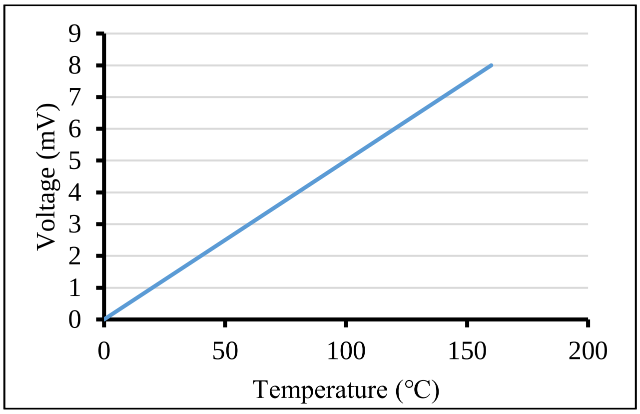


**Figure 2.** Sample of the calibration results of the thermocouples

The fins are made of plates with 0.5 mm thickness, 0.5, 0.7, and 1.0 mm in height and 0.5 mm in width. The distance between fins is 1 mm. The fins are attached to both ends of the hater holder. A water pump to circulate water inside the coiled tube. The copper tube serves to exchange heat between inside and outside fluids. The tube is spirally wrapped and pre-connected to a pump. The measuring devices used were low-cost microcontroller-based temperature sensors in the sink, the heater, the condensing system, and the inlet and outlet temperatures of the condensation tube. Surface-mounted sensors are used to detect cool-down functions in the evaporator system, known as evaporation value. Hybrid nanoparticles of $Al_2O_3$ with CuO and ZnO were measured in weight percentages of 0.1 to 0.4 wt.%, 0.25 to 0.25 wt.%, and 0.4 to 0.1 wt.%. The material's thermal and physical properties are shown in Table 1.

Hybrid fluid equations reported by Shamshirgaran et al. [18] have been used to predict the physical properties, and then the masses that should be used in the tests were calculated.

The use of the nanomaterial ZnO has a convincing reason for use. Through the properties in Table 1, the strength of the physical properties in thermal transfer is observed. Therefore, it is necessary to use it to confirm the comparison process in nanomaterials. The roughness of micro fins is 60 micrometers. Table 2 presents the case selection.

**Table 2.** Tested cases of compositions

| Case | Composition |
|---|---|
| Case-1 | Water + 0.1 wt% $Al_2O_3$ + 0.4 wt% CuO |
| Case-2 | Water + 0.25 wt% $Al_2O_3$ + 0.25 wt% CuO |
| Case-3 | Water + 0.4 wt% $Al_2O_3$ + 0.1 wt% CuO |
| Case-4 | Water + 0.1 wt% $Al_2O_3$ + 0.4 wt% ZnO |
| Case-5 | Water + 0.25 wt% $Al_2O_3$ + 0.25 wt% ZnO |
| Case-6 | Water + 0.4 wt% $Al_2O_3$ + 0.1 wt% ZnO |

2.1.2 Experimental procedure

• A constant temperature was added, as the test was done by taking the processor out of the tank and then heating it to a temperature of 150°C.

• Maintaining this temperature due to the presence of a relay system to control the stability of the temperature to be set.

• Then, the test section was immersed inside the tank to obtain a critical heat flux.

### 2.2 Numerical procedure

Numerical simulations and experimental tests will be used in this integration. In fact, it is hard to simulate condensation and evaporation at the same time, so each process should have its connected domain.

2.2.1 Model generation

The actual boiling will be simulated on the one hand, and the results of boiling and the percentage degree of moisture will be transferred later to the other hand, which is represented by the condensation process to obtain appropriate results Figure 3.

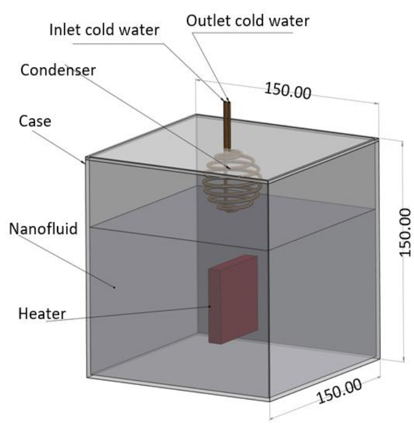


**Figure 3.** Computational model with all geometries in mm

2.2.2 Mesh generation and independency checking

Unstructured grids perform well for complicated geometries and make use of the tetrahedral grid method in this study. In ANSYS version 19.0, a single input can provide output in terms of the mesh through its solid geometry or model. Herein, the collection of a total of 4.8×106 cells was carried out, as indicated in Figure 4.

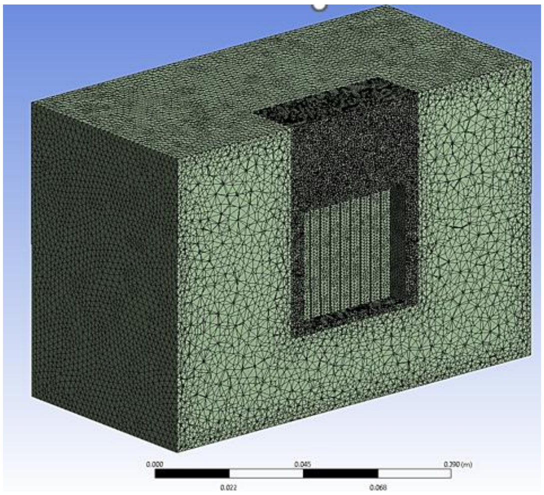


**Figure 4.** Meshing scheme of the computational model

The solution of the matrix domain equations involves the implementation of complex algorithms that make a correct mesh requirement. Following that, it would investigate the reliability of a mesh in order to achieve a final steady state of outcomes. 4804515 was assigned to the element when the maximum temperature was 418.2 K from Table 3.

**Table 3.** Mesh independency

| Case | Element | Node | Max. Temperature (K) |
|---|---|---|---|
| 1 | 1323509 | 498468 | 425.8 |
| 2 | 2613460 | 608456 | 419.9 |
| 3 | 3725444 | 723409 | 418.4 |
| 4 | 4804515 | 877918 | 418.2 |

2.2.3 Assumptions and boundary conditions

- Transient-state
- Condition
- Incompressible fluid
- Negligible radiation heat transfer
- No electromagnetic field influence
- Laminar flow

For the lower part, a temperature of 150°C was inserted into the processor body, and the surface of the lower part was used as an outlet with a pressure of 0 Pa. As for the upper part, the exit velocity of the upper part was entered as the velocity inlet, the temperature of the upper part, as well as the volume fraction values.

2.2.4 Governing equations

To illustrate the improvement of pool boiling heat transfer by using $Al_2O_3$ and micro fins and hybrid nanomaterials. The basic pool boiling of heat transfer can be described by the following general equation [15]:

$$q = h_{\mathrm{pb}} \cdot \Delta T \tag{1}$$

where, $q$ is the heat flux (W/m$^2$), $h_{\mathrm{pb}}$ is the pool boiling heat transfer coefficient (W/m$^2$·K), and $\Delta T$ is the temperature difference between the heating surface and the bulk liquid (K).

a. Micro-fins in the simulation

Micro fins can enhance heat transfer by increasing the effective surface area for boiling. This enhancement can be incorporated by modifying the heat transfer coefficient [15]:

$$h_{\mathrm{pb}} = h_{\mathrm{base}} + \frac{k_{\mathrm{fins}} \cdot A_{\mathrm{fiss}}}{V} \tag{2}$$

where, $h_{\mathrm{base}}$ is the base heat transfer coefficient without fins (W/m$^2$·K), $k_{\mathrm{fins}}$ is the thermal conductivity of the fins (W/m·K), $A_{\mathrm{fins}}$ is the total surface area of the fins (m$^2$), and $V$ is the volume of the boiling liquid (m$^3$).

b. Nanomaterials in the simulation

Using water-based nanomaterials that are made of $Al_2O_3$ nanoparticles prevents the thermo property of the solution from being changed and, hence, affects heat transfer. The increase in heat transfer resistance may be conveyed as the change in heat transfer coefficient [15].

$$h_{\mathrm{pb}} = h_{\mathrm{base}} + \frac{k_{\mathrm{mandinid}}\, \Delta T}{L} \tag{3}$$

where, $k_{\mathrm{nanofluid}}$ is the effective thermal conductivity of the nanofluid (W/m·K), $\Delta T$ is the temperature difference between the heating surface and the bulk nanofluid ($K$), and $L$ is the characteristic length scale (m).

c. The combined effect of hybrid nanomaterials and micro-fins

Combining the effects of micro fins and nanomaterials, the total pool boiling heat transfer coefficient can be expressed as [15]:

$$h_{\mathrm{pb,total}} = h_{\mathrm{base}} + \frac{k_{\mathrm{fins}} \cdot A_{\mathrm{finks}}}{V} + \frac{k_{\mathrm{amanofluid}} \cdot \Delta T}{L} \tag{4}$$

This equation captures the synergistic effects of both micro fins and nanomaterials on enhancing pool boiling heat transfer.

These equations serve for both numerical ways of learning the pool boiling process with the mixed nanomaterials that consist of $Al_2O_3$ and micro fins, and thus, experiments. The particular coefficients and factors require experimentation and numerical analysis.

d. Numerical formulation

The CFD model should solve the following fundamental equations. The governing equations are solved using the ANSYS program [19]:

Continuity equation:

$$\frac{\partial \rho}{\partial t} + \nabla \cdot (\rho \mathrm{u}) = 0 \tag{5}$$

Momentum equation:

$$\frac{\partial (\rho \mathrm{u})}{\partial t} + \nabla \cdot (\rho \mathrm{uu}) = -\nabla p + \nabla \cdot (\mu \nabla \mathrm{u}) + \mathrm{F} \tag{6}$$

Energy equation:

$$\frac{\partial(\rho E)}{\partial t}+\nabla\cdot(\mathrm{u}(\rho E+p))=\nabla\cdot(k\nabla T)+S_E \quad (7)$$

$S_E$ represents energy sources (e.g., heat flux due to phase change).

Nanofluids are engineered by dispersing nanoparticles into a base fluid, which alters its thermal properties. The effective properties can be calculated using mixture models:

Effective density [16, 18]:

$$\rho_{\text{eff}}=(1-\phi)\rho_f+\phi\rho_p \quad (8)$$

Effective specific heat [16, 18]:

$$C_{p,\text{eff}}=(1-\phi)C_{p,f}+\phi C_{p,p} \quad (9)$$

Effective thermal conductivity [16, 18]:

$$k_{\text{eff}}=k_f\left[\frac{k_p+2k_f-2\phi(k_f-k_p)}{k_p+2k_f+\phi(k_f-k_p)}\right] \quad (10)$$

Effective viscosity [16, 18]:

$$\mu_{\text{eff}}=\mu_f(1+2.5\phi) \quad (11)$$

where, $\phi$ is the volume fraction of nanoparticles. Subscripts $f$ and $p$ denote the base fluid and particle properties, respectively.

In ANSYS, the heat transfer coefficient $h$ can be applied as a boundary condition in thermal analysis. The heat transfer coefficient is typically used in convective heat transfer scenarios and can be defined using the following basic equation for convective heat transfer:

$$q=h\cdot A\cdot(T_{\text{surface}}-T_\infty) \quad (12)$$

### 2.3 Uncertainty analysis calculation

2.3.1 Instrumental uncertainty calculation

Each measuring device has a specified uncertainty. Using the root sum square method:

$$U_i=[(U_T)^2+(U_q)^2+(U_p)^2]^{0.5} \quad (13)$$

2.3.2 Uncertainty in heat transfer coefficient

The heat transfer coefficient is derived from:

$$h=\frac{q}{\Delta T} \quad (14)$$

Applying error propagation:

$$U_h=\sqrt{\left(\frac{U_q}{q}\right)^2+\left(\frac{U_T}{T}\right)^2} \quad (15)$$

Using typical values, the uncertainty in the heat transfer coefficient is $\pm 5.03\%$.

2.3.3 Mesh independence study (numerical uncertainty)

From the grid convergence index (GCI):

$$GCI=\frac{|E_f-E_c|}{E_c}\times 100\% \quad (16)$$

where:

- $E_f$ = Fine mesh solution
- $E_c$ = Coarse mesh solution

2.3.4 Final uncertainty estimation

Combining experimental and numerical uncertainties:

$$U_{\text{total}}=\sqrt{U_h^2+U_{\text{GCI}}^2} \quad (17)$$

## 3. RESULTS AND DISCUSSION

All results obtained through the simulation software and from the experimental side will be reviewed with respect to the different concentrations of the hybrid nanomaterials used and the use of the fins. The instrumental uncertainty is ±2.07%. The numerical uncertainty is ±0.4%. The final uncertainty in the results is ±5.05%.

### 3.1 Experimental results

Combination nanomaterials in the structure of micro fins show an increase in the heat transfer coefficient and a decrease in critical heat flux, contributing to better heat removal and extending the operation period. On the one hand, they have suitable conditions in the experiment, but on the other, they can influence uniform dispersion, stability, and reproducibility. Generally, hybrid nanomaterials are the machinery for bettering heat transfer performance, stability, and durability in micro fin boiling thermal exchange. However, well-designed experimental studies should be carried out to prove their applicability and clarify their underlying mechanisms.

Figure 5 shows the temperature sensor at pin2 in the upper area. It is noted that the temperature value in the case of WAC0.1 reached 34.8°C. In the case WAC0.25, the temperature reached 35.4°C, and in the case of WAC0.4, the temperature reached 35.9°C. The best case is using hybrid nanomaterials using CuO.

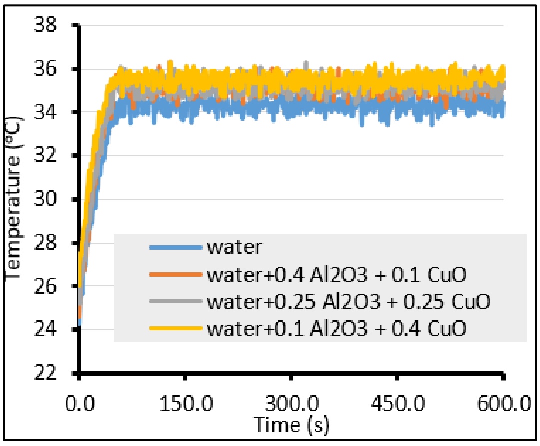


**Figure 5.** Temperature with time at pin 2 with micro fins 5 mm at different concentrations of hybrid nanomaterials $Al_2O_3$ with CuO

Figure 6 shows the temperature sensor at pin2 in the upper area at various concentrations. It is noted that the temperature value in the case WAZ0.1 reached 35.6°C. In the case of WAZ0.25, the temperature reached 35.8°C, and in the case of WAZ0.4, the temperature reached 36.3°C. The best case is using hybrid nanomaterials using ZnO.

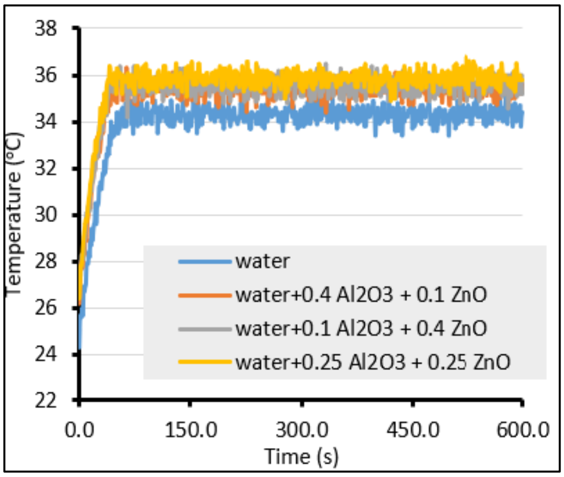


**Figure 6.** Temperature with time at pin 2 with micro fins 5 mm at different concentrations of hybrid nanomaterials $Al_2O_3$ with ZnO

Figure 7 shows the temperature sensor at pin5 in the bottom area at various times. It is noted that the temperature value in the case WAC0.1 reached 65°C. In the case of WAC0.25, the temperature reached 66°C, and in the case of WAC0.4, the temperature reached 67°C. The best case is using hybrid nanomaterials using CuO.

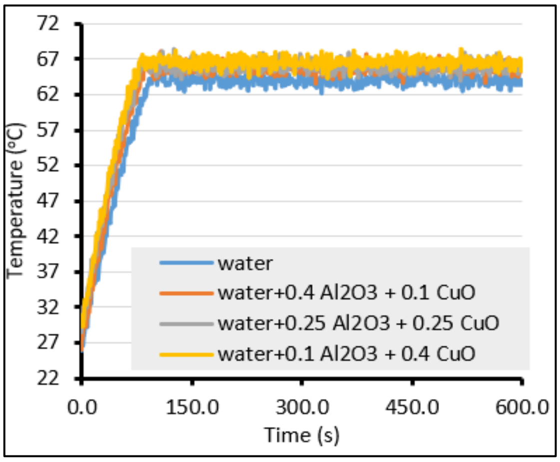


**Figure 7.** Temperature with time at pin 5 with micro fins 5 mm at different concentrations of hybrid nanomaterials $Al_2O_3$ with CuO

Figure 8 shows the temperature sensor at pin5 in the bottom area at various concentrations of nanofluids. It is noted that the temperature value in the case WAZ0.1 reached 64°C. In the case of WAZ0.25, the temperature reached 66°C, and in the case of WAZ0.4, the temperature reached 68°C. The best case is using hybrid nanomaterials using ZnO.

Figure 9 shows the percentage of humidity in the upper point at pin8. The humidity value reached 93% in the case of WAC0.1, in the case of WAC0.25, it reached 94%, and in the case of WAC0.4, it reached 95%. This shows the importance of using nanomaterials. In thermal discharge from the copper tube to the humid air surrounding it.

Figure 10 shows the percentage of humidity in the upper point pin8. The humidity value reached 94% in the case of WAZ0.1, in the case of WAZ0.25, it reached 96%, and in the case of WAZ0.4, it reached 98%. This shows the importance of using nanomaterials in thermal discharge processes from the copper tube to the humid air surrounding it.

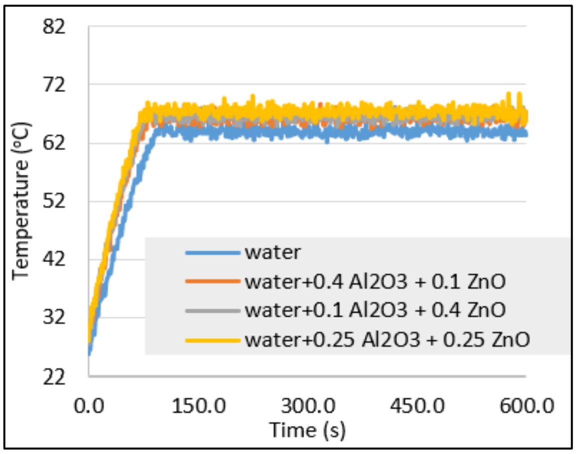


**Figure 8.** Temperature variation with time at pin 5 with micro fins 5 mm at different concentrations of hybrid nanomaterials $Al_2O_3$ with ZnO

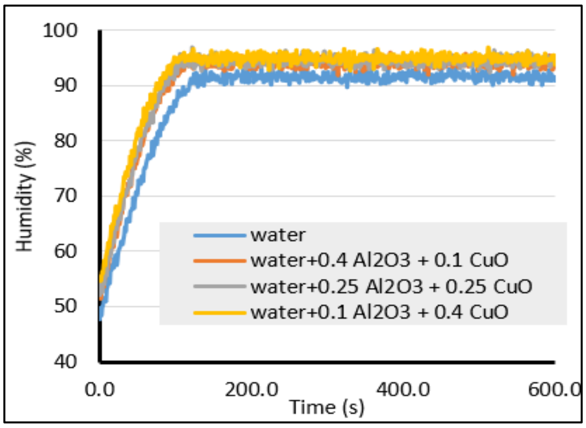


**Figure 9.** Humidity with time at pin 8 with micro fins 5 mm at different concentrations of hybrid nanomaterials $Al_2O_3$ with CuO

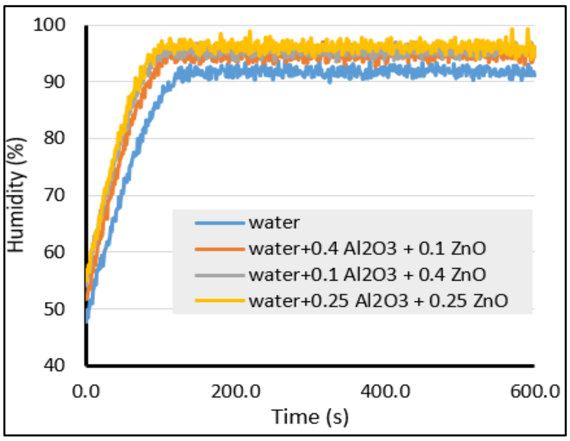


**Figure 10.** Humidity variation with time at pin 8 with micro fins 5 mm at different concentrations of hybrid nanomaterials $Al_2O_3$ with ZnO

### 3.2 Validation

Reddy and Venkatachalapathy [20] focused on the enhancement of thermal properties and critical heat flux (CHF) by mixing two different nanoparticles, viz., alumina and copper oxide, at various concentrations in Deionized (DI) water. Volume concentrations of 0.01-0.1% were prepared and the stability of nanofluids is confirmed by Zeta potential. The thermal conductivity of hybrid nanofluids was enhanced by 15.72% for 0.1% concentration at room temperature compared with DI water. CHF of hybrid nanofluids was always higher than single-type nanofluids. Maximum enhancement of 49.84% in CHF was obtained for 0.1% concentration. HTC was enhanced by 7.1 and 6.72% for 0.01 and 0.03% volume concentrations than DI water and started decreasing with increasing volume concentrations. A comparison of results presented in Figure 11 showed great convergence between the previous and current works, and the difference did not exceed 5% of the error rate.

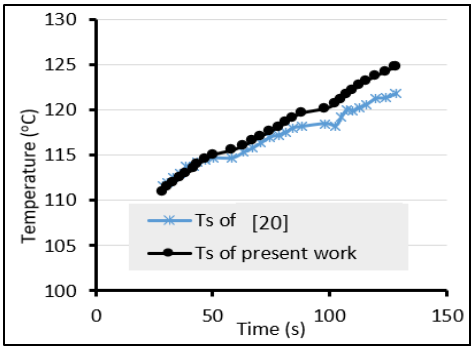


**Figure 11.** Temperature distribution of surface between previous work (Reddy and Venkatachalapathy [20]) and present work

Mehralizadeh et al. [1] conducted research on surface modifications to enhance nucleation sites. The micro-fins in the work validate that surface modifications create major effects on heat transfer. The research conducted by Mahmoud and Karayiannis [3] examined boiling surface enhancements but identified performance evaluation difficulties because of surface roughness and fluid dynamics mechanics. The experimental and numerical evidence led to a stronger analysis than previous studies. Sharma et al. [5] discovered that Ag/ZnO nanofluids enhanced heat transfer coefficients (HTC) and critical heat flux (CHF) but resulted in decreased efficiency at elevated concentrations. The researchers from Qi et al. [15] verified that $TiO_2$ nanofluids boosted boiling heat transfer by 77.7% during low-concentration usage yet showed decreasing performance at increased ratios. The experimental findings with $Al_2O_3$-CuO and $Al_2O_3$-ZnO hybrid nanoparticles demonstrate that proper nanoparticle combination selection produces essential outcomes.

### 3.3 Simulation results

The joining of different Nanoparticles or structures to enhance properties creates Nano-hybrid materials. They can improve the surface area, wettability, and thermal conductivity and thereby enhance the efficiency of heat transfer in pool boiling heat transfer with micro fins. They can also lower thermal resistance, avoid the formation of surface fouling, regulate bubble dynamics, and attain temperature uniformity. The particular advantages are determined by the kind of nanomaterials used, their combination with micro fins as well as by the system operating conditions. The introduction of nanoparticles such as carbon nanotubes or graphene into these nanomaterials allows for better heat dissipation and decreased thermal resistance, thus improving the overall heat transfer performance. However, the type of nanomaterials used, their combination, and operating parameters determine the particular advantages.

3.3.1 Effect of the hybrid nano on the bottom enclosure

In Figure 12, which shows the distribution of temperatures across the lower region using hybrid nanomaterials, it is noted that increasing the amount of CuO concentrations increases the temperature of the liquid and the thermal discharge from the fins as the region surrounding the fins reaches 34℃ in the case WAC0.1, while in the case WAC0.25. Temperatures reached 35℃, and in this case, WAC0.4 temperatures reached 38℃.

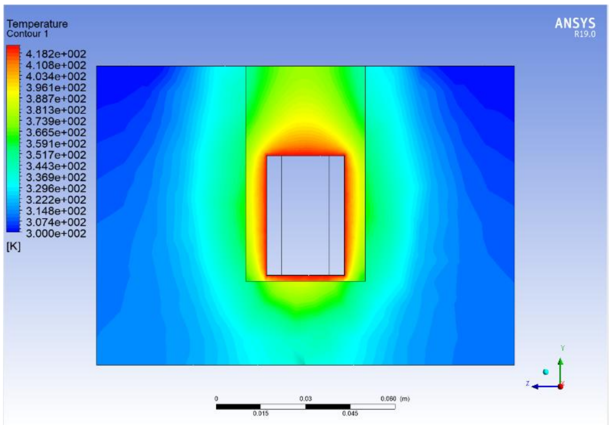


(a)

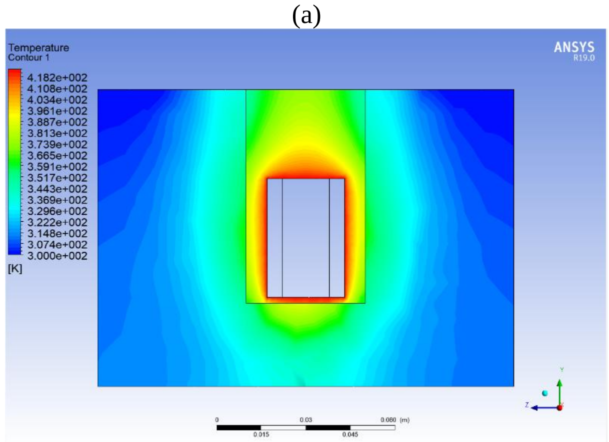


(b)

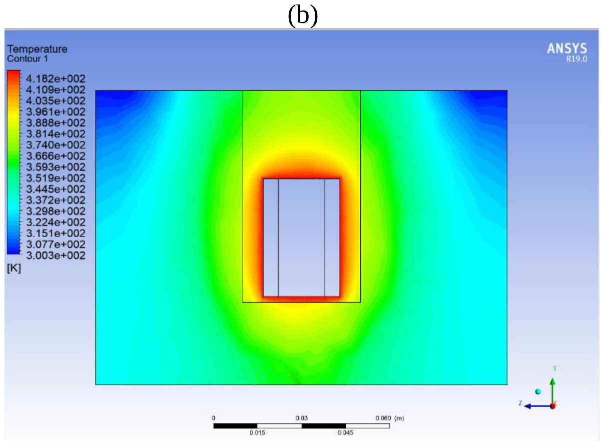


(c)

**Figure 12.** Temperature contour of the heater in the pool for boiling process in the bottom zone with micro fins 5 mm at different concentrations of hybrid nanomaterials: (a) WAC0.1, (b) WAC0.25, (c) WAC0.4

As for Figure 13, which shows the boiling process, it shows that the addition of hybrid nanomaterials increases the generation of the resulting steam. Which accordingly increases the heat exchange process, as the volume fraction in the case WAC0.1 reached 0.407, while in the case WAC0.25, it reached 0.436, while in the case WAC0.4 reached 0.7794, and this indicates the effectiveness of using nanomaterials in thermal discharge.

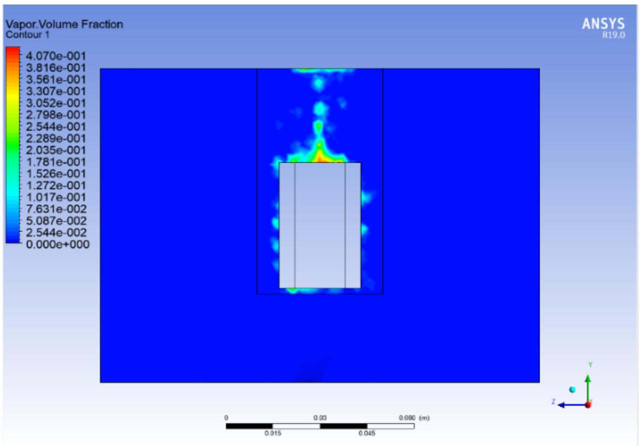


(a)

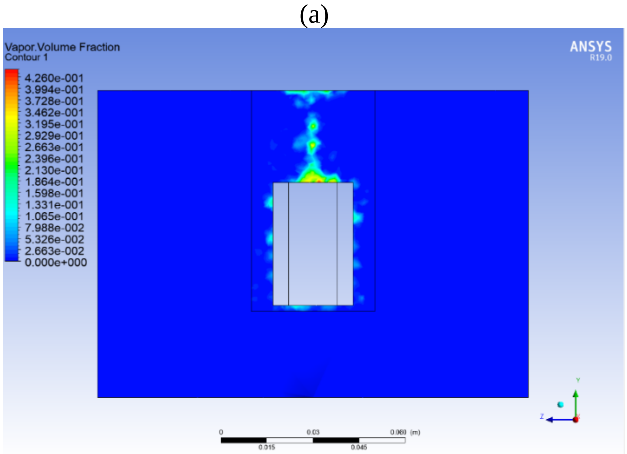


(b)

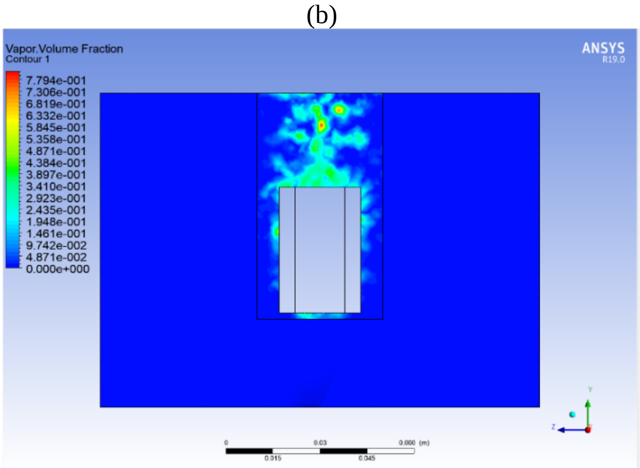


(c)

**Figure 13.** The volume of fraction contour of the heater in the pool for the boiling process in the bottom zone with micro fins 5 mm at different concentrations of hybrid nanomaterials: (a) WAC0.1, (b) WAC0.25, (c) WAC0.4

Figure 14 shows the distribution of temperatures across the lower region using hybrid nanomaterials. It is noted that increasing the amount of ZnO concentrations increases the temperature of the liquid and the thermal discharge from the fins. The region surrounding the fins reached 36°C in the case WAZ0.1, while in the case WAZ0.25. Temperatures reached 38°C, and in this case, WAZ0.4 temperatures reached 40°C.

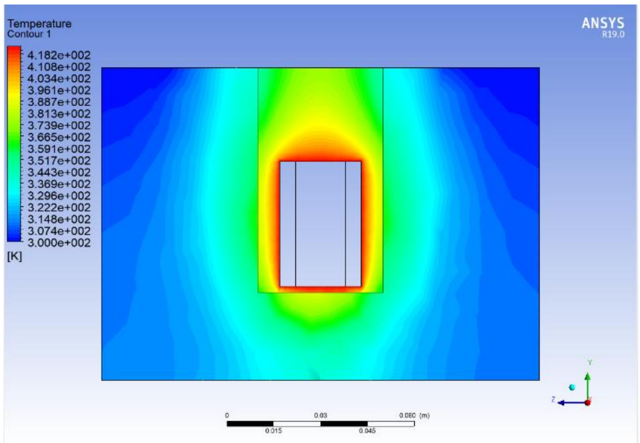


(a)

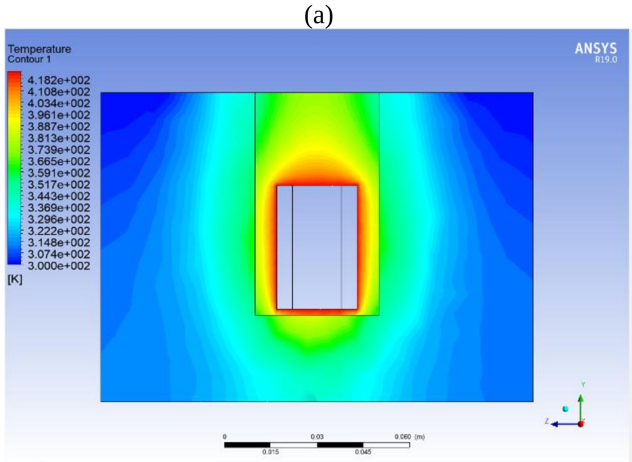


(b)

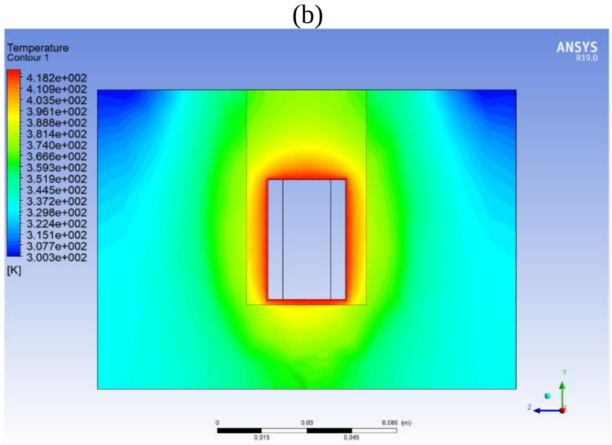


(c)

**Figure 14.** Temperature contour of the heater in the pool for boiling process in the bottom zone with micro fins 5 mm at different concentrations of hybrid nanomaterials: (a) WAZ0.1, (b) WAZ0.25, (c) WAZ0.4

Figure 15 shows the boiling process, and it shows that the addition of hybrid nanomaterials increases the generation of the resulting steam, which accordingly increases the heat exchange process. The volume fraction in the case WAZ0.1 reached 0.407, while in the case WAZ0.25, it reached 0.524, while in the case WAZ0.4 reached 0.598, and this indicates the effectiveness of using nanomaterials in thermal discharge.

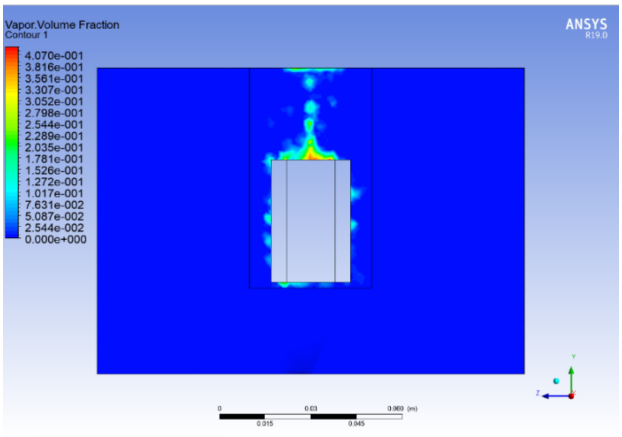


(a)

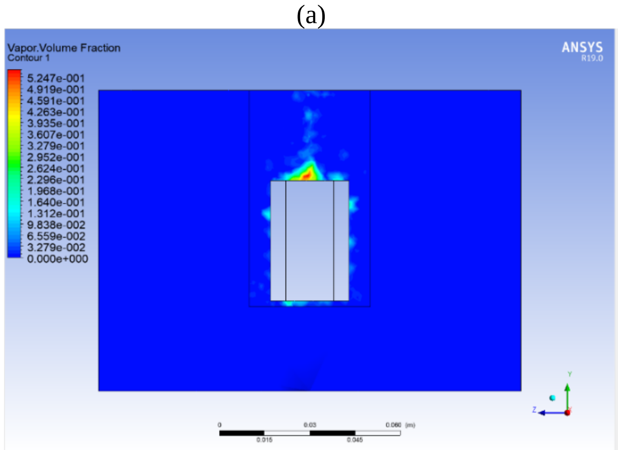


(b)

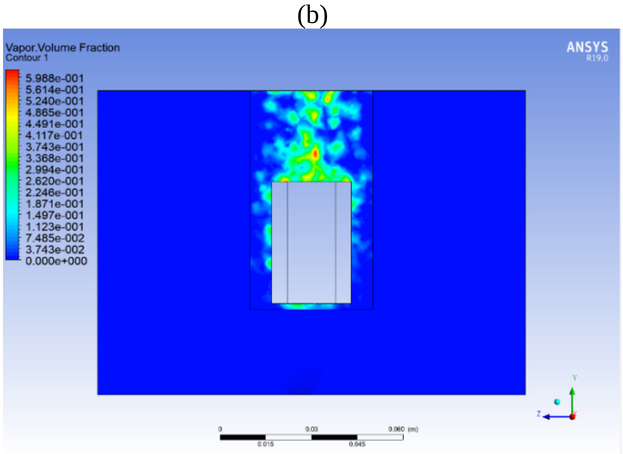


(c)

**Figure 15.** The volume of fraction contour of the heater in the pool for the boiling process in the bottom zone with micro fins 5 mm at different concentrations of hybrid nanomaterials: (a) WAZ0.1, (b) WAZ0.25, (c) WAZ0.4

3.3.2 Effect of the hybrid nanoadditives on the top enclosure

As for Figure 16, which shows the upper area of the condensation process, it is noted that the temperature in the case of WAC0.1 reached 66°C. In the case of WAC0.25, the temperature reached 74°C. In the case of WAC0.4, the temperature reached 73°C, and this indicates improvement. This is evident in the use of hybrid nanomaterials.

Figure 17, where the most important phase of the condensation process is in the upper section and the formation of condensed water, shows that the amount of condensed water rises with the rise of the percentage of hybrid nanomaterials. The temperature of the fluid increases with the increase in the concentration of CuO.

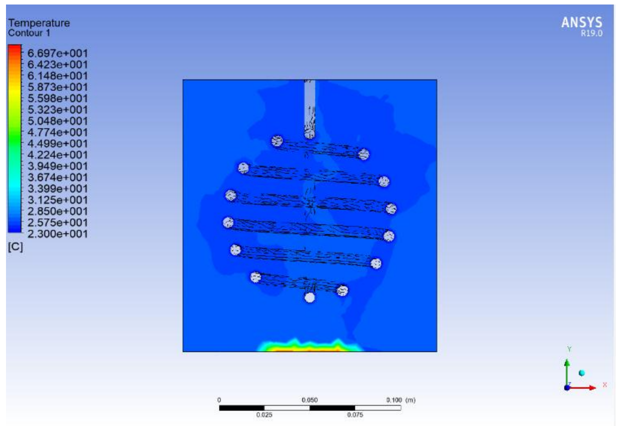


(a)

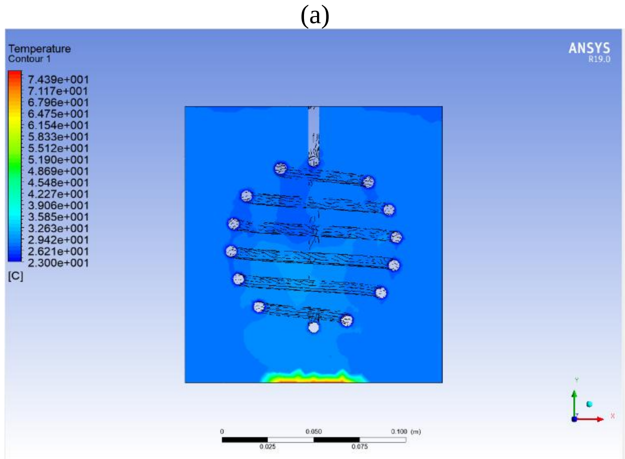


(b)

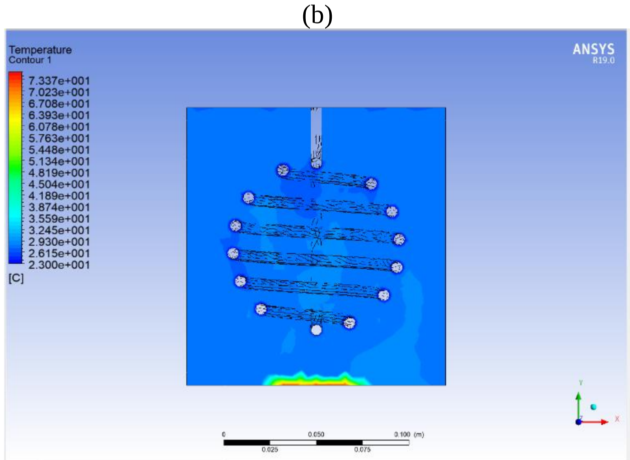


(c)

**Figure 16.** Temperature contour of the heater in the pool for boiling process in the top zone with micro fins 5 mm at different concentrations of hybrid nanomaterials: (a) WAC0.1, (b) WAC0.25, (c) WAC0.4

Figure 18 shows the upper area of the condensation process, and it is noted that the temperature in the case WAZ0.1 reached 77°C. In the case of WAZ0.25, the temperature reached 80°C. In the case WAZ0.4, the temperature reached 75°C, and this indicates improvement. This is evident in the use of hybrid nanomaterials.

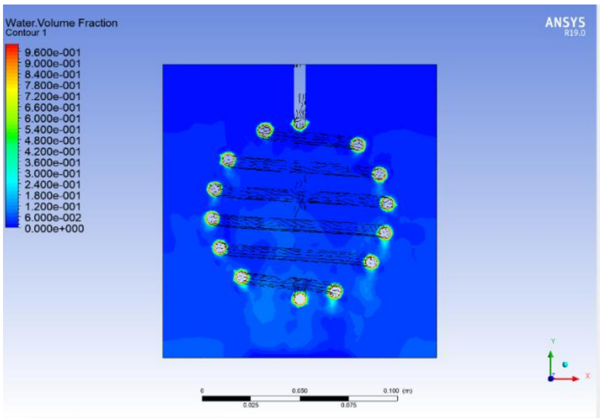


(a)

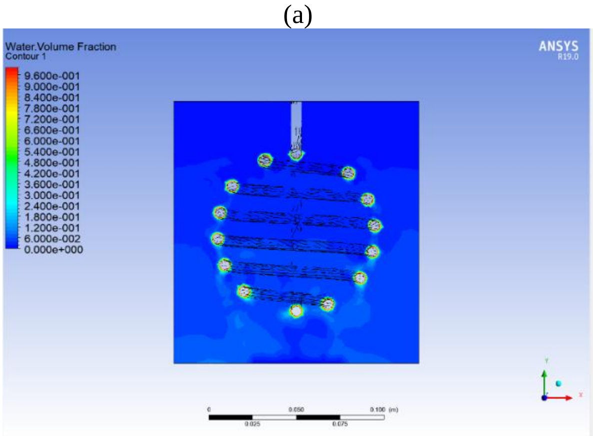


(b)

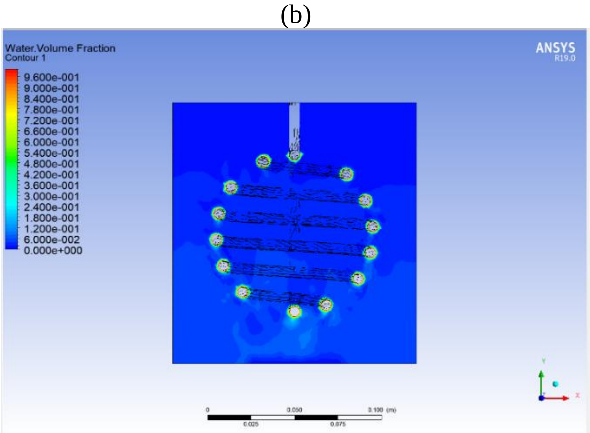


(c)

**Figure 17.** The volume of fraction contour of the heater in the pool for the boiling process in the top zone with micro fins 5 mm at different concentrations of hybrid nanomaterials: (a) WAC0.1, (b) WAC0.25, (c) WAC0.4

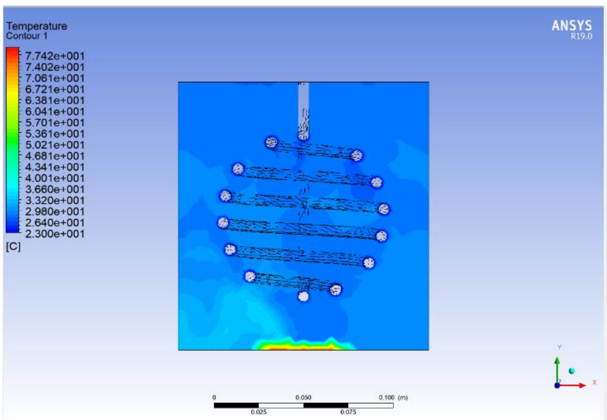


(a)

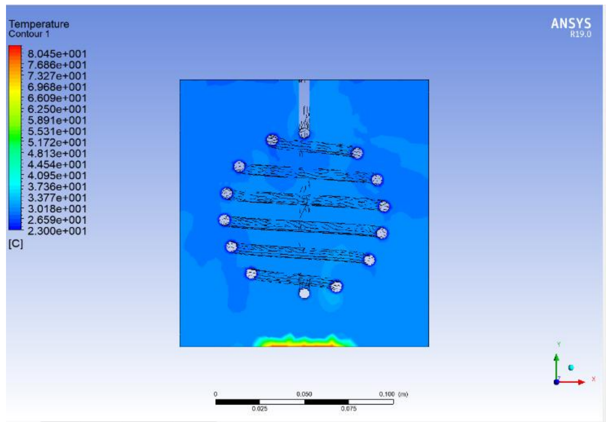


(b)

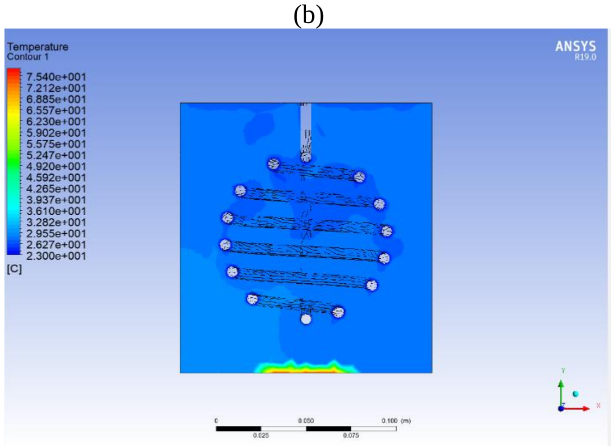


(c)

**Figure 18.** Temperature contour of the heater in the pool for boiling process in the top zone with micro fins 5 mm at different concentrations of hybrid nanomaterials: (a) WAZ0.1, (b) WAZ0.25, (c) WAZ0.4

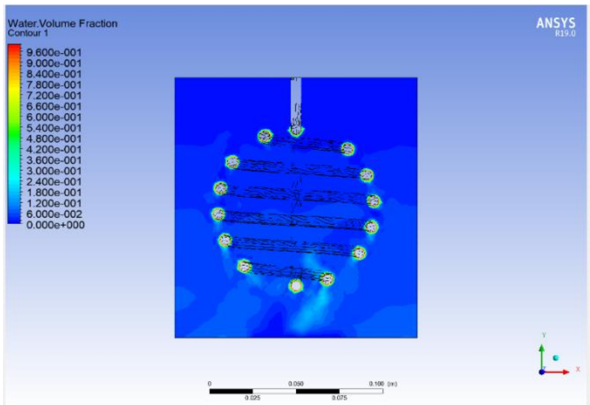


(a)

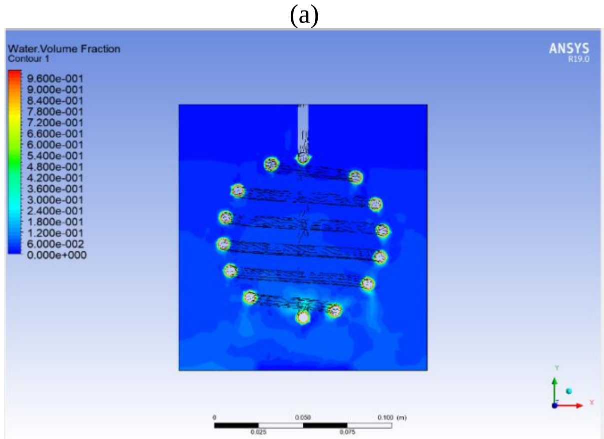


(b)

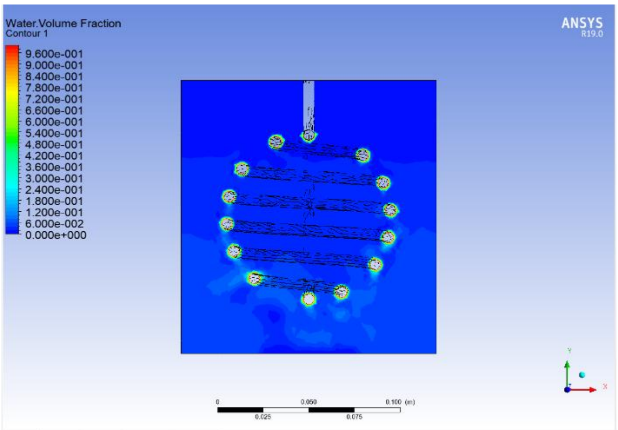


(c)

**Figure 19.** The volume of fraction contour of the heater in the pool for the boiling process in the top zone with micro fins 5 mm at different concentrations of hybrid nanomaterials: (a) WAZ0.1, (b) WAZ0.25, (c) WAZ0.4

In Figure 19, which shows the condensation process in the upper section and the formation of condensed water, it is noted that the amount of condensed water increases with the increase in the percentage of hybrid nanomaterials.

## 4. CONCLUSIONS

The paper focuses on the study of the pool boiling heat transfer efficiency with the help of hybrid nanofluids like $Al_2O_3$ and micro fins. It combines numerical analysis and simulation to determine the optimal design parameters. They constructed the pool with an acrylic shell, installed copper tubing for the heating and waterproofing system, and surveyed it with a microcontroller system. The findings could be concluded in the following.

- The temperature of the liquid in the heat sink depends on CuO concentrations; therefore, with an increase in CuO concentrations, the probable temperature in the surrounding region will also increase.
- The insertion of nanomaterials increases the rate of steam production, which improves heat exchange. According to the materials, the thermal discharge demonstrates an effective method.
- Although the condensation of water is combined with the hybrid nanomaterials, it is seen that the process is actually more effective when the temperatures are in the range of 66, 74, and 73°C. The main step is a drop formation in amount with regard to the number of components considering the ionic ratio for the hybrid nanomaterials. The temperature of the condensation process also increases as height increases and is at 77°C at the highest range, 80°C at the middle range, and 75°C at the highest range, which illustrates the advancement of the process.
- The upper area was sent the water, Alumina ($Al_2O_3$), CuO, and ZnO temperature through pin2 thermal sensor temperature. Of all the cases, hybrid samples of CuO and ZnO nanomaterials are the best, with their temperatures of 34.8, 35.8, and 36.3°C, respectively, the highest. Having established when these compounds could be best used after increasing the temperature to its optimal level, it was clear that the best two were CuO and ZnO.

## REFERENCES

[1] Mehralizadeh, A., Shabanian, S.R., Bakeri, G. (2020). Effect of modified surfaces on bubble dynamics and pool boiling heat transfer enhancement: A review. Thermal Science and Engineering Progress, 15: 100451. https://doi.org/10.1016/j.tsep.2019.100451

[2] Mukherjee, S., Ebrahim, S., Mishra, P.C., Ali, N., Chaudhuri, P. (2022). A review on pool and flow boiling enhancement using nanofluids: Nuclear reactor application. Processes, 10(1): 177. https://doi.org/10.3390/pr10010177

[3] Mahmoud, M.M., Karayiannis, T.G. (2021). Pool boiling review: Part II – Heat transfer enhancement. Thermal Science and Engineering Progress, 25: 101023. https://doi.org/10.1016/j.tsep.2021.101023

[4] Gajghate, S.S., Barathula, S., Cardoso, E.M., Saha, B.B., Bhaumik, S. (2021). Effect of staggered V-shaped and rectangular grooves copper surfaces on pool boiling heat transfer enhancement using $ZrO_2$ nanofluids. Journal of the Brazilian Society of Mechanical Sciences and Engineering, 43: 1-23. https://doi.org/10.1007/s40430-020-02759-8

[5] Sharma, P.O., Barewar, S.D., Chougule, S.S. (2021). Experimental investigation of heat transfer enhancement in pool boiling using novel Ag/ZnO hybrid nanofluids. Journal of Thermal Analysis and Calorimetry, 143: 1051-1061. https://doi.org/10.1007/s10973-020-09922-2

[6] Ravi Babu, S., Saras Chandra, A., Ramesh Babu, P. (2021). Recent developments in synthesis, characterization and boiling heat transfer of nanofluids - A review. IOP Conference Series: Materials Science and Engineering, 1033: 012072. https://doi.org/10.1088/1757-899X/1033/1/012072

[7] Moghadasi, H., Saffari, H. (2021). Experimental study of nucleate pool boiling heat transfer improvement utilizing micro/nanoparticles porous coating on copper surfaces. International Journal of Mechanical Sciences, 196: 106270. https://doi.org/10.1016/j.ijmecsci.2021.106270

[8] Dadhich, M., Prajapati, O.S., Sharma, V. (2021). A systematic review on the heat transfer investigation of the flow boiling process. Chemical Engineering and Processing - Process Intensification, 165: 108425. https://doi.org/10.1016/j.cep.2021.108425

[9] Moghadasi, H., Malekian, N., Saffari, H., Gheitaghy, A.M., Zhang, G.Q. (2020). Recent advances in the critical heat flux amelioration of pool boiling surfaces using metal oxide nanoparticle deposition. Energies, 13(15): 4026. https://doi.org/10.3390/en13154026

[10] Soleimani, A., Sattari, A., Hanafizadeh, P. (2020). Thermal analysis of a microchannel heat sink cooled by two-phase flow boiling of $Al_2O_3$ HFE-7100 nanofluid. Thermal Science and Engineering Progress, 20: 100693. https://doi.org/10.1016/j.tsep.2020.100693

[11] Mukesh Kumar, P.C., Arun Kumar, C.M. (2020). Numerical study on heat transfer performance using $Al_2O_3$/water nanofluids in six circular channel heat sink for electronic chip. Materials Today: Proceedings, 21: 194-201. https://doi.org/10.1016/j.matpr.2019.04.220

[12] Mehralizadeh, A., Shabanian, S.R., Bakeri, G. (2020). Experimental and modeling study of heat transfer enhancement of $TiO_2/SiO_2$ hybrid nanofluids on modified surfaces in pool boiling process. The European Physical Journal Plus, 135: 796.

https://doi.org/10.1140/epjp/s13360-020-00809-7
[13] Khan, S.A., Atieh, M.A., Koç, M. (2018). Micro-nano scale surface coating for nucleate boiling heat transfer: A critical review. Energies, 11(11): 3189. https://doi.org/10.3390/en11113189
[14] Das, S., Kumar, V., Gajghate, S.S., Bhaumik, S. (2017). Nucleate pool boiling heat transfer on micro/nano composite porous surfaces. In Proceedings of the International Conference on Mechanical Engineering, Bangaluru, India.
[15] Qi, C., Wan, Y., Liang, L., Rao, Z., Li, Y. (2016). Numerical and experimental investigation into the effects of nanoparticle mass fraction and bubble size on boiling heat transfer of $TiO_2$-water nanofluid. Journal of Heat Transfer, 138(8): 081503. https://doi.org/10.1115/1.4033353
[16] Jaswal, R., Sathyabhama, A., Singh, K., Yandapalli, A.V.V.R.P. (2023). Experimental and numerical investigation of pool boiling heat transfer from finned surfaces. Applied Thermal Engineering, 233: 121167. https://doi.org/10.1016/j.applthermaleng.2023.121167
[17] Alshuhail, L.A. (2023). Pool boiling heat transfer characteristics of using nanofluids. Materials Research Proceedings, 36: 47-55. https://doi.org/10.21741/9781644902790-5
[18] Shamshirgaran, S.R., Al-Kayiem, H.H., Sharma, K.V., Ghasemi, M. (2020). State of the art of techno-economics of nanofluid-laden flat-plate solar collectors for sustainable accomplishment. Sustainability, 12(21): 9119. https://doi.org/10.3390/su12219119
[19] ANSYS. (n.d.). Engineering simulation software. http://ansys.com.
[20] Reddy, Y.A., Venkatachalapathy, S. (2018). Heat transfer enhancement studies in pool boiling using hybrid nanofluids. Thermochimica Acta, 672: 93-100. https://doi.org/10.1016/j.tca.2018.11.014

## NOMENCLATURE

| | |
|---|---|
| $q$ | heat flux, W/m$^2$ |
| $h$ | pool boiling heat transfer coefficient, W/(m$^2$·K) |
| $\Delta T$ | the temperature difference between the heating surface and bulk liquid, K |
| $h_0$ | base heat transfer coefficient without fins, W/(m$^2$·K) |
| $k_f$ | thermal conductivity of the fins, W/(m·K) |
| $A_f$ | total surface area of the fins, m$^2$ |
| $V_l$ | the volume of the boiling liquid, m$^3$ |
| $k_{eff}$ | effective thermal conductivity of nanofluid, W/(m·K) |
| L | characteristic length scale, m |
| $\rho$ | density, k |
| Cp | specific heat capacity, g/m$^3$ |
| $\phi$ | volume fraction of nanoparticles, J/(kg·K) |
| $\mu$ | dynamic viscosity, Pa·s |
| u | velocity vector, m/s |
| p | pressure, Pa |
| F | body forces (e.g., gravity), N |
| E | total energy, J |
| T | temperature, K |